

Dynamics of brain function in patients with chronic pain assessed by microstate analysis of resting-state electroencephalography

Elisabeth S. May^{a,b}, Cristina Gil Ávila^{a,b}, Son Ta Dinh^{a,b}, Henrik Heitmann^{a,b,c}, Vanessa D. Hohn^{a,b}, Moritz M. Nickel^{a,b}, Laura Tiemann^{a,b}, Thomas R. Tölle^{a,c}, Markus Ploner^{a,b,c,*}

Abstract

Chronic pain is a highly prevalent and severely disabling disease that is associated with substantial changes of brain function. Such changes have mostly been observed when analyzing static measures of resting-state brain activity. However, brain activity varies over time, and it is increasingly recognized that the temporal dynamics of brain activity provide behaviorally relevant information in different neuropsychiatric disorders. Here, we therefore investigated whether the temporal dynamics of brain function are altered in chronic pain. To this end, we applied microstate analysis to eyes-open and eyes-closed resting-state electroencephalography data of 101 patients suffering from chronic pain and 88 age- and sex-matched healthy controls. Microstate analysis describes electroencephalography activity as a sequence of a limited number of topographies termed microstates that remain stable for tens of milliseconds. Our results revealed that sequences of 5 microstates, labelled with the letters A to E, consistently described resting-state brain activity in both groups in the eyes-closed condition. Bayesian analysis of the temporal characteristics of microstates revealed that microstate D has a less predominant role in patients than in controls. As microstate D has previously been related to attentional networks and functions, these abnormalities might relate to dysfunctional attentional processes in chronic pain. Subgroup analyses replicated microstate D changes in patients with chronic back pain, while patients with chronic widespread pain did not show microstates alterations. Together, these findings add to the understanding of the pathophysiology of chronic pain and point to changes of brain dynamics specific to certain types of chronic pain.

Keywords: Chronic pain, Dynamics, EEG, Microstate analysis, Resting-state

1. Introduction

Chronic pain is a highly disabling disease that affects 20% to 30% of the adult population.^{7,24} Its pathophysiology is not fully understood, and treatment is often insufficient,⁶⁰ imposing a tremendous burden on patients, health care systems, and society.⁴⁶ Converging lines of evidence have shown that chronic pain is associated with extensive changes of brain structure and function.^{2,29} Understanding these changes promises fundamental insights into the underlying

pathophysiology and might eventually help to establish a much sought-after biomarker of chronic pain.^{14,58}

Brain function in chronic pain has mostly been assessed using functional magnetic resonance imaging (fMRI)² and electroencephalography (EEG)/magnetoencephalography.⁴⁴ Most studies have analyzed static measures of brain activity during the resting state, usually by aggregating a certain feature of brain function across several minutes. However, brain activity varies over time, and it is increasingly recognized that these temporal dynamics provide behaviorally and clinically relevant information that complements static measures.^{19,45} Correspondingly, it has been proposed that the dynamics of brain activity and connectivity critically shape the perception of pain.²⁸ By assessing brain activity and connectivity at ultra-low frequencies below 0.1 Hz, recent fMRI studies have provided support for this concept in chronic pain.^{3,5,10,59} However, the temporal dynamics of chronic pain-related brain activity at frequencies higher than 1 Hz have not been consistently explored yet.

Electroencephalography and magnetoencephalography are well suited to study such dynamic changes of brain activity at higher frequencies. One of the best-established methods in this field is microstate analysis (see Refs. 25,34 for reviews) that has revealed that temporal changes of EEG activity do not occur randomly. Instead, EEG activity switches between a limited number of so-called microstates. During a microstate, the EEG topography remains stable for tens of milliseconds before abruptly transitioning to another microstate. Electroencephalography resting-state activity is usually well-described with 4 to 6 microstates, which are remarkably similar across participants. Thus, microstate analysis quantifies resting-state EEG recordings

Sponsorships or competing interests that may be relevant to content are disclosed at the end of this article.

E.S. May and C. Gil Ávila contributed to this work equally.

^a Department of Neurology, School of Medicine, Technical University of Munich (TUM), Munich, Germany, ^b TUM-Neuroimaging Center, School of Medicine, TUM, Munich, Germany, ^c Center for Interdisciplinary Pain Medicine, School of Medicine, TUM, Munich, Germany

*Corresponding author. Address: Department of Neurology, Technical University of Munich (TUM), Ismaninger Str. 22, 81675 Munich, Germany. Tel.: +49-89-4140-4608. E-mail address: markus.ploner@tum.de (M. Ploner).

Supplemental digital content is available for this article. Direct URL citations appear in the printed text and are provided in the HTML and PDF versions of this article on the journal's Web site (www.painjournalonline.com).

PAIN 162 (2021) 2894–2908

Copyright © 2021 The Author(s). Published by Wolters Kluwer Health, Inc. on behalf of the International Association for the Study of Pain. This is an open access article distributed under the terms of the Creative Commons Attribution-Non Commercial-No Derivatives License 4.0 (CCBY-NC-ND), where it is permissible to download and share the work provided it is properly cited. The work cannot be changed in any way or used commercially without permission from the journal.

<http://dx.doi.org/10.1097/j.pain.0000000000002281>

as sequences of a limited number of microstates. The temporal characteristics of these microstates carry important information about mental processes.^{6,34} Moreover, abnormalities of temporal microstate characteristics have been observed in different neuropsychiatric disorders.^{12,38,48} During the writing of this article, a first microstate study in patients suffering from chronic pain was published. The results showed lower occurrence and time coverage of microstate C in patients with chronic widespread pain.²⁰ However, these findings need to be replicated and extended to other chronic pain conditions.

Here, we investigated whether the temporal dynamics of brain activity are changed in a large cohort of patients suffering from chronic pain. To this end, we applied microstate analysis to EEG resting-state recordings of 101 patients suffering from different types of chronic pain and 88 matched healthy control participants. Thereby, the study aimed to further the understanding of the pathophysiology of chronic pain and to potentially contribute to the development of a brain-based biomarker of chronic pain.

2. Materials and methods

2.1. Participants

The current study represents a re-analysis of previously published data obtained at the Technical University of Munich for the large-scale study of brain dysfunction in chronic pain.⁵⁴ One hundred one patients (69 women; age = 58.1 ± 13.6 years [mean \pm SD]) suffering from different types of chronic pain and 88 age- and sex-matched healthy controls (60 women, age = 57.5 ± 14.2 years) participated in the study. Inclusion criteria for patients were a clinical diagnosis of chronic pain, with pain lasting at least 6 months, and a minimum reported average pain intensity of at least 4 of 10 during the past 4 weeks (0 = no pain and 10 = worst imaginable pain). Exclusion criteria for patients were acute changes of the pain condition during the past 3 months (eg, due to recent injuries or surgeries), major neurological diseases (eg, epilepsy, stroke, or dementia), major psychiatric diseases aside from depression, and severe general diseases. Patients taking benzodiazepines were also excluded. Other medication was not restricted and was maintained. In total, 47 patients with chronic back pain, 30 patients with chronic widespread pain, 6 patients with joint pain, and 18 patients with neuropathic pain were included in the study. Exclusion criteria for healthy participants were a medical history of pain lasting more than 6 months, having any pain on the day of testing, surgery, or acute injury during the past 3 months, and any neurological or psychiatric diseases. All participants provided written informed consent. The study was approved by the ethics committee of the Medical Faculty of the Technical University of Munich and conducted according to the relevant guidelines and regulations.

Questionnaires were used to assess pain characteristics and comorbidities immediately before the EEG recording. All patients completed the following questionnaires: Pain characteristics were assessed by the short-form McGill Pain Questionnaire (SF-MPQ),³³ depression by the Beck Depression Inventory II (BDI-II),⁴ and anxiety by the State-Trait Anxiety Inventory (STAI).⁵² The medication was quantified for all patients using the Medication Quantification Scale (MQS),²¹ which quantifies a patient's pain medication profile in a single numerical value. Eighty-one patients additionally completed the painDETECT questionnaire¹⁸ to assess the neuropathic pain component, and 47 patients completed the Pain Disability Index (PDI)¹⁶ and the Veteran's RAND 12-Item Health Survey (VR-12)⁵⁰ to assess pain disability and quality of life, respectively. All healthy control participants completed BDI-II and STAI questionnaires to

assess potential comorbidities. Detailed characteristics of the participants can be found in **Table 1**.

2.2. Recordings

Brain activity was recorded using EEG during the resting state. Participants were instructed to stay in a wakeful and relaxed state without performing any particular task. For most participants, two 5-minute blocks of continuous resting-state data were recorded, one with eyes closed and the other with eyes open. During the eyes-open condition, participants were asked to rest their gaze on a centrally presented visual fixation cross. The temporal order of the blocks was counterbalanced. During the recording, participants were comfortably seated and listened to white noise played through headphones to mask any ambient noise. For 5 patients with chronic widespread pain and 7 healthy controls, only one 5-minute block with eyes closed was recorded. Thus, final sample sizes were 101 patients and 88 healthy controls for the eyes-closed condition and 96 patients and 81 healthy controls for the eyes-open condition.

Data were recorded with 64 electrodes and a BrainAmp MR plus amplifier (Brain Products, Munich, Germany). The electrodes included all electrodes from the International 10-20 system and the additional electrodes Fpz, CPz, POz, Oz, Iz, AF3/4, F5/6, FC1/2/3/4/5/6, FT7/8/9/10, C1/2/5/6, CP1/2/3/4/5/6, TP7/8/9/10, P1/2/5/6/7/8, and PO3/4/7/8/9/10 (Easycap, Herrsching, Germany). Two electrodes were placed below the outer canthus of each eye to monitor eye movements. All EEG electrodes were referenced to electrode FCz and grounded at electrode AFz. For 81 patients and 69 healthy controls, muscle activity was simultaneously recorded with 2 bipolar electromyography (EMG) electrode montages and a BrainAmp ExG MR amplifier (Brain Products, Munich, Germany). Electromyography electrodes were placed on the right masseter and neck (semispinalis capitis and splenius capitis) muscles.¹³ The EMG ground electrode was placed at vertebra C2. Data were obtained at a sampling frequency of 1000 Hz, with 0.1- μ V resolution, and were band-pass filtered online between 0.016 and 250 Hz. Impedances were kept below 20 k Ω .

2.3. Preprocessing

Preprocessing was performed with the Brain Vision Analyzer software (Brain Products, Munich, Germany) on the appended data from the eyes-open and the eyes-closed conditions. For artifact identification, a high pass filter at 1 Hz and a notch filter at 50 Hz were applied to remove low frequency drifts and electrical line noise, respectively. Independent component analysis was performed.²³ Components representing eye movements and muscle artifacts were identified based on their time courses and topographies and subtracted from the raw unfiltered EEG time series.⁶¹ Signal jumps higher than $\pm 100 \mu$ V and their adjacent time intervals (200 ms before and after the jump) were marked for rejection. Subsequently, all data sets were visually inspected, and remaining bad intervals were marked for rejection. Finally, data were re-referenced to the average reference, and the reference electrode FCz was added to the electrode array.

2.4. Microstate analysis

Microstate analysis was performed using the free academic software Cartool version 3.8,⁹ MATLAB (MathWorks, Natick, MA), and the MATLAB toolbox Fieldtrip.⁴¹ Analyses were performed separately for the eyes-open and eyes-closed

Table 1
Demographic data and questionnaire results.

	Patients with chronic pain (mean ± SD)	Healthy controls (mean ± SD)
Number	101	88
Sex (m/f)	32/69	28/60
Age (y)	58.2 ± 13.5	57.5 ± 14.3
BDI	15.8 ± 8.9	3.5 ± 4.5
STAI—state	39.5 ± 10.6	30.6 ± 6.1
STAI—trait	44.0 ± 11.2	30.9 ± 7.1
SF-MPQ total pain score	27.1 ± 9.4	—
Current pain intensity (0-10)	5.2 ± 1.9	—
Avg. pain intensity in the past 4 wk (0-10)	5.6 ± 1.6	—
Pain duration (mo)	121.8 ± 114.4	—
PDQ	17.4 ± 6.5	—
PDI	27.4 ± 14.2	—
VR-12 PCS	31.8 ± 7.8	—
VR-12 MCS	46.4 ± 11.9	—
MQS	6.8 ± 8.1	—

Please note that data for avg. pain intensity in the past 4 weeks, pain duration, and PDQ were only available for a subset of 81 patients. Data from PDI, VR-12 PCS, and VR-12 MCS were only available for a subset of 47 patients. For most patients (n = 81), current pain intensity ratings were obtained from the painDETECT questionnaire, which uses a combination of numerical rating scale anchored at 0 (no pain) and 10 (max pain) with a color gradient. For n = 20 patients with chronic widespread pain, current pain intensity ratings were obtained from the SF-MPQ, which uses a visual analogue scale anchored at 0 (no pain) and 100 (worst imaginable pain). These ratings were divided by 10 to match rating scales across questionnaires.

Avg. pain intensity, average pain intensity in the past 4 weeks; BDI, Beck Depression Inventory; MQS, medication quantification scale; PDI, pain disability index; PDQ, painDETECT questionnaire; STAI, State-Trait Anxiety Inventory; SF-MPQ, Short-form McGill Pain Questionnaire; VAS, visual analogue scale; VR-12 PCS, Veteran's RAND 12-Item Physical Component Summary; VR-12 MCS, Veteran's RAND 12-Item Mental Component Summary.

conditions. Each 5-minute recording was first band-pass filtered between 1 and 40 Hz and downsampled to 125 Hz, in line with previous studies.^{8,11,56} Subsequently, intervals marked as bad during preprocessing were rejected, and microstate analysis was performed using all remaining clean segments concatenated. An overview of the microstate analysis pipeline can be found in **Figure 1**.

2.4.1. Definition of microstates

We defined microstates through a well-established 2-step clustering procedure using a modified k-means algorithm.⁴² In line with previous studies,^{12,38,48,55} this was performed separately for each group and condition.

The first step consisted of a k-means clustering performed at the individual level. For each participant, EEG topographies at global field power (GFP) peaks were clustered, yielding a variable number of individual-level topographies. The GFP is a measure of the instantaneous strength of EEG activity measured over the whole scalp and mathematically defined as the SD of the signals of all electrodes.³⁹ EEG topographies were clustered at GFP maxima since they represent the time points of highest signal-to-noise ratio.^{39,42}

The clustering algorithm requires an a priori definition of k, which is the number of clusters into which the data will be grouped. To select the optimal number of clusters, we performed the clustering with different numbers of k = 1 to 12 initial clusters, following Cartool default settings for resting-state data. First, an initial number of k topographies was randomly selected from all GFP-peak topographies of the individual EEG time series. Second, the selected topographies were spatially correlated with the remaining topographies at GFP peaks, ignoring polarity. The spatial correlation is a scalar value computed as the Pearson correlation coefficient between all matched electrodes of 2 different topographies.³⁹ Third, the topographies at GFP peaks

were assigned to the cluster with the highest spatial correlation. If the highest correlation was smaller than 0.5 in absolute value (ie, in the range of -0.5 to 0.5), the topography was not assigned to any cluster. This threshold represents a trade-off between rejecting too many and too few topographies during labelling and was chosen in line with previous studies^{6,11,63} and the Cartool default settings. Fourth, the center of each cluster was computed, resulting in k new “average” cluster topographies. The new cluster topographies were then again correlated with the topographies at GFP peaks, closing the loop. The algorithm stopped when the variance of the clusters converged to a limit. To overcome the random selection of the initial cluster topographies, the clustering was repeated 100 times per set of k clusters and the set explaining most variance of the data was selected. The optimal number of clusters was identified for each individual separately according to a meta-criterion with 7 independent optimization criteria (for more details refer to Ref. 6). This procedure resulted in 4 to 8 topographies for each participant and condition.

In the second step, a second k-means clustering was performed at group level, clustering the concatenated individual topographies obtained in the previous step. For the second clustering, an initial number of k = 4 to 15 clusters and 200 k-means initializations were set. Again, the polarity was ignored, and a maximum absolute Pearson correlation coefficient higher than 0.5 was needed for cluster assignment. The same meta-criterion as before was used to identify the optimal number of clusters on a group level.

This 2-step clustering is a nondeterministic algorithm and can thus yield varying results when repeated. To assess the reliability of our findings, we repeated the entire procedure for the definition of group microstates 5 times for both the eyes-closed and the eyes-open conditions. The identified optimal numbers of group microstates were then compared across reruns. For the eyes-closed condition, the optimal number of group microstates

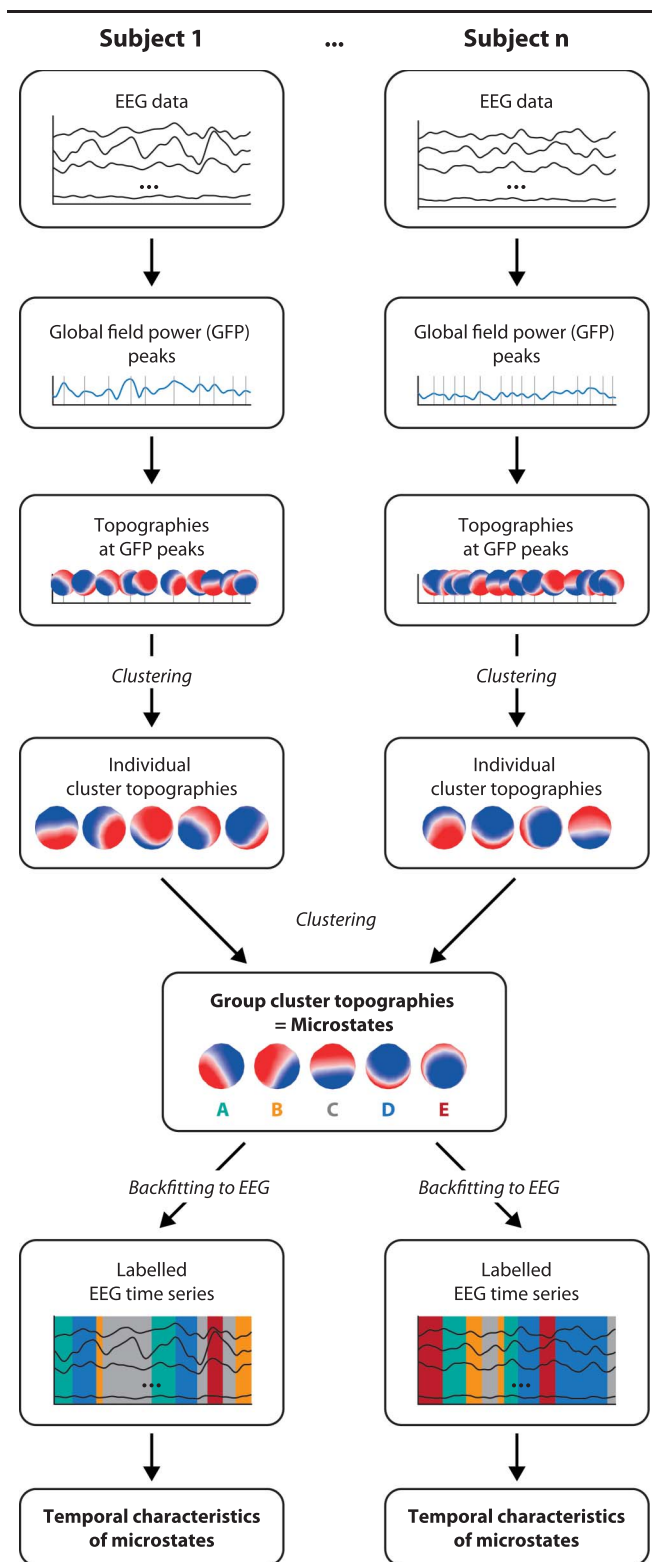


Figure 1. Microstate analysis. For each participant, the global field power (GFP) is calculated and topographies at GFP peaks are selected for individual clustering. Topographies at GFP peaks are clustered with a modified k-means clustering, leading to a variable number of individual cluster topographies per individual. Next, individual cluster topographies are concatenated and clustered on a group level. This consistently resulted in 5 different group cluster topographies for the eyes-closed condition, labelled as microstates A to E. Microstate topographies are then fitted back to the individual EEG data, resulting in a labelled EEG time series in which each time point is associated to a microstate. From the labelled EEG time series, the temporal characteristics of microstates are derived. This analysis was performed separately per group (patients with chronic pain and healthy controls). EEG, electroencephalography.

showed considerable stability (eyes-closed; number of microstates for 5 reruns for patients/controls: 5, 5, 5, 4, 5/5, 5, 5, 5, 5). For the eyes-open condition, by contrast, the optimal number of group microstates strongly varied across reruns, especially for patients, and could not reliably be estimated (eyes-open; number of microstates for 5 reruns for patients/controls: 5, 6, 4, 6, 5/5, 5, 5, 4, 5). See Supplementary Figure 1 for a depiction of group-level microstates for all reruns (available at <http://links.lww.com/PAIN/B351>). In light of this lack of reliability in the eyes-open condition, all further analyses were restricted to the eyes-closed condition (see below for a discussion of potential reasons for this discrepancy).

Group microstates of a representative rerun of the eyes-closed condition are shown in **Figure 2A**. Results of this rerun will be exemplarily shown throughout the article. To show the reliability of the findings, analyses of the other 4 eyes-closed reruns are also summarized in the article and their detailed results are shown in the supplementary material (available at <http://links.lww.com/PAIN/B351>). Topographies were visually inspected and compared with topographies reported in the literature. For both groups, the first 4 topographies closely resembled the 4 well-known “canonical” microstates A to D reported previously and were labeled accordingly.^{25,27,34} The topography of the fifth microstate closely resembled a microstate that has been consistently reported in more recent studies,^{6,11,63} since an increasing number of studies is now using a data-driven approach to define the optimal number of microstates. We labeled it with the letter E. Throughout the article, these 5 group-level topographies are referred to as microstates A to E. Similarities and differences of microstate topographies between groups were assessed by calculating spatial correlations and topographic analyses of variance (TANOVAs) for all microstates (A to E), respectively. Topographic analysis of variance is a nonparametric randomization test based on the global map dissimilarity of individual topographies.³⁹ The global map dissimilarity is a measure of the difference between 2 topographies directly related to the spatial correlation.³⁹ For each microstate, global map dissimilarity was computed between the microstate topographies of the patient and control groups using Cartool.⁹ To obtain a *P*-value, this dissimilarity was compared with a distribution of dissimilarities, which was generated by randomly shuffling individual topographies between patient and controls and re-computing the dissimilarity between the center topographies of the randomized groups. The process was repeated 5000 times. This comparison resulted in a *P*-value per microstate, which was given by the proportion of permutations in which the dissimilarity was smaller than the dissimilarity originally observed in the data. Resulting *P*-values were corrected for multiple comparisons across the 5 microstate classes using the resampling-based false discovery rate (FDR).⁶² Adjusted *P*-values are reported.

2.4.2. Temporal microstate characteristics

Next, we determined the temporal characteristics of the 5 microstates for both groups. To this end, individual EEG time series were construed as time series of microstates through a “fitting procedure,” that is, a microstate was assigned to every time point. For each participant, the EEG topographies of all time points were spatially correlated to the microstate topographies of the participant’s group (patients/controls) using absolute Pearson correlation coefficients. Next, each EEG time point was assigned to a microstate (A to E). To ensure a certain continuity in the microstate time series, the relabeling was performed based

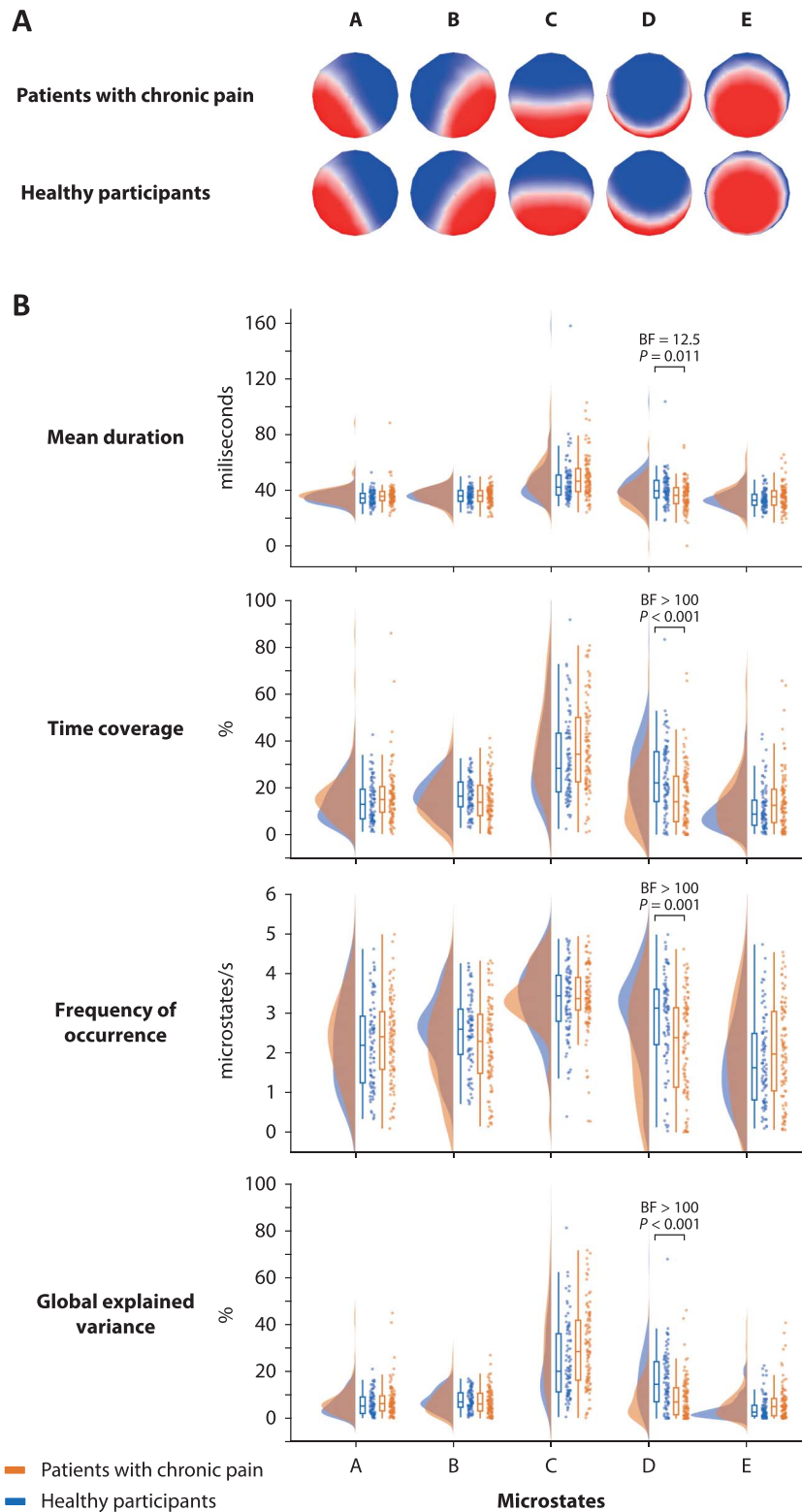


Figure 2. Microstate topographies and their temporal characteristics for all patients with chronic pain ($n = 101$) compared with healthy controls ($n = 88$) in the eyes-closed condition (representative rerun). (A) Microstate topographies were defined for the entire mixed chronic pain group and healthy controls separately. Microstates were labelled with the letters A to E according to previous literature.³⁴ (B) Temporal characteristics. Mean duration, time coverage, frequency of occurrence, and global explained variance of each microstate were calculated for each participant. Raincloud plots¹ show unmirrored violin plots displaying the probability density function of the data, boxplots, and individual data points. Boxplots depict the sample median as well as first (Q1) and third quartiles (Q3). Whiskers extend from Q1 to the smallest value within $Q1 - 1.5 \times$ interquartile range (IQR) and from Q3 to the largest values within $Q3 + 1.5 \times$ IQR. BF, Bayes factor in favor of the alternative hypothesis.

on 2 criteria: (1) the correlation should be high, and (2) most surrounding time points should belong to the same microstate.⁹ To fulfill this compromise between goodness of fit and smoothness, standard temporal smoothing (window half size = 5 and strength (Besag factor) = 10) was applied.^{42,55} No label was assigned if the highest (absolute) spatial correlation was smaller than 0.5. On average, the percentage of unlabeled time points was smaller than 0.1% and no differences existed between groups (representative rerun: $\text{mean}_{\text{patients}} = 0.080\%$, $\text{mean}_{\text{controls}} = 0.095\%$, $t = 0.630$, $P = 0.530$, $\text{BF}_{10} = 0.190$, median $\delta = 0.085$, 95% credible interval = $[-0.190 \text{ to } 0.362]$; two-sided independent-samples t tests).

Based on the time series of microstates, 4 measures were calculated to quantify the temporal characteristics of each microstate: mean duration, time coverage, frequency of occurrence, and global explained variance. The mean duration is the average time (in milliseconds) for which a microstate persists before transitioning to a different microstate. The time coverage is the percentage of total time that a microstate is present. The frequency of occurrence is the number of times that a microstate recurs per second. The global explained variance is the percentage of global variance that is explained by every microstate.

Temporal characteristics of microstates were determined for all 5 reruns of the eyes-closed condition. As outlined above, the meta-criterion indicated a number of 5 microstates for both groups for all but 1 rerun, for which it indicated 4 optimal group-level microstates for patients. To enable a comparison of temporal characteristics between groups for this rerun, temporal characteristics were determined for the 5-microstate solution of the microstate analysis. Results of the representative rerun can be found in **Figure 2B**, results for all other reruns in Supplementary Table 1 (available at <http://links.lww.com/PAIN/B351>).

Finally, we investigated the microstate sequence by examining the transition probabilities from each microstate to the others for the representative rerun.^{31,40,55} To this end, we computed the matrix of transition counts among all microstates for each participant and divided it by the overall count of transitions.

2.5. Statistical analysis

Group differences of temporal microstate measures (mean duration, time coverage, frequency of occurrence, and global explained variance) and transition probabilities were analyzed in JASP version 0.13.1²² using 2-sided independent-samples t tests in both frequentist and Bayesian frameworks. For the frequentist approach, significance level was set to 0.05. For P -values of temporal measures, resampling-based FDR correction⁶² was performed in MATLAB (MathWorks, Natick, MA) across the 5 microstates and the 4 different temporal measures, resulting in a correction for 20 statistical tests per rerun. Adjusted P -values⁶² are reported throughout the article. For the transition matrix of the representative rerun, FDR correction was performed across all 20 transitions. For the Bayesian analysis, default priors (Cauchy distributions with a scale parameter $r = 0.707$) were used. In addition to t -values and FDR-adjusted P -values, results are reported using the two-tailed Bayes factor BF_{10} . Effect size estimates for the BF_{10} are reported as the median of the posterior δ distribution together with its 95% credibility interval.

Finally, we investigated relationships between temporal microstate measures and clinical parameters for the representative rerun using JASP version 0.13.1.²² To this end, temporal microstate measures of microstate D (mean duration, time coverage, frequency of occurrence, and global explained

variance) were selected for a correlation analysis, since they consistently showed significant differences between patients and controls across all reruns. Pearson correlations were calculated between the microstate measures and major clinical parameters that were available for all patients (current pain intensity, SF-MPQ total pain score, depression [BDI], and medication [MQS]). Please note that for most patients ($n = 81$), current pain intensity ratings were obtained from the painDETECT questionnaire, which uses a combination of a numerical rating scale anchored at 0 (no pain) and 10 (max pain) with a color gradient. Twenty patients with chronic widespread pain did not complete painDETECT questionnaires. For these patients, current pain intensity ratings were obtained from the SF-MPQ, which uses a visual analogue scale anchored at 0 (no pain) and 100 (worst imaginable). These ratings were divided by 10 to match rating scales across questionnaires. Correlations were again calculated in both frequentist and Bayesian frameworks. In the Bayesian analysis, default priors (stretched beta priors with width = 1) were used. Results are reported using the Pearson correlation coefficient, its FDR-adjusted P -value, its Bayes factor (BF_{10}), and the 95% credibility interval of the correlation coefficient. FDR correction of P -values⁶² was performed in MATLAB (MathWorks, Natick, MA) across all 16 performed correlations.

2.6. Subgroup analyses

Finally, we investigated whether the results could be replicated within particular patient subgroups of our mixed sample. To this end, we repeated the definition of microstates and the investigation of their temporal characteristics in the eyes-closed condition for the 2 largest subgroups: patients with chronic back pain and patients with chronic widespread pain. These 2 groups were chosen based on the sample size. With a medium effect size Cohen's d of 0.5 and a type 1 error of 0.05, a post hoc power analysis revealed a power of 0.78 and 0.65 for 2-sided independent-samples t tests comparing our healthy control group ($n = 88$) with the chronic back pain ($n = 47$) and chronic widespread pain ($n = 30$) patient groups, respectively. For patients with neuropathic pain ($n = 18$) and joint pain ($n = 6$), power was even lower (0.48 and 0.29, respectively). Thus, microstate analysis was repeated for patients with chronic back pain and chronic widespread pain only. Individual topographies of each patient subgroup were selected for a new second clustering to obtain subgroup-specific microstate topographies. Subgroup-specific temporal characteristics were obtained through back-fitting and were statistically compared with the temporal characteristics of the healthy control group for each patient group as described above. Again, 5 reruns of these subgroup analyses were performed to assess the reliability of findings. For each subgroup, a representative rerun is shown in the article, and details of additional reruns are presented in the supplementary material (available at <http://links.lww.com/PAIN/B351>).

2.7. Data and code availability

Electroencephalography data in BIDS format⁴³ as well as scripts for statistical analyses are openly available at <https://osf.io/srpbq/>.

3. Results

The current study investigated whether the dynamics of resting-state brain activity are altered in patients suffering from chronic pain. We performed microstate analysis, which describes the

Table 2

Comparisons of temporal microstate measures for all patients with chronic pain (n = 101) compared with healthy controls (n = 88) in the eyes-closed condition (representative rerun).

Microstate	Measure	t	P	BF ₁₀	Median effect size (δ)	95% CI
A	Mean dur.	−1.947	0.132	0.919	−0.265	−0.547 to 0.012
	Time cov.	−1.586	0.167	0.510	−0.216	−0.496 to 0.061
	Freq. of occ.	−0.809	0.471	<i>0.215</i>	−0.110	−0.387 to 0.166
	GEV	−1.635	0.167	0.548	−0.222	−0.503 to 0.055
B	Mean dur.	0.491	0.656	<i>0.177</i>	0.067	−0.209 to 0.343
	Time cov.	1.583	0.167	0.507	0.215	−0.062 to 0.495
	Freq. of occ.	2.316	0.072	1.892	0.317	0.037 to 0.600
	GEV	0.801	0.471	<i>0.214</i>	0.109	−0.167 to 0.386
C	Mean dur.	−1.356	0.230	0.373	−0.184	−0.463 to 0.092
	Time cov.	−1.777	0.154	0.686	−0.242	−0.523 to 0.035
	Freq. of occ.	−0.285	0.775	<i>0.164</i>	−0.039	−0.315 to 0.237
	GEV	−2.441	0.062	2.482	−0.334	−0.618 to 0.054
D	Mean dur.	3.087	0.011	12.530	0.425	0.142 to 0.711
	Time cov.	4.010	<0.001	>100	0.556	0.268 to 0.847
	Freq. of occ.	3.803	0.001	>100	0.526	0.240 to 0.816
	GEV	5.220	<0.001	>100	0.730	0.436 to 1.027
E	Mean dur.	−1.575	0.167	0.501	−0.214	−0.494 to 0.063
	Time cov.	−1.856	0.144	0.783	−0.253	−0.534 to 0.025
	Freq. of occ.	−1.333	0.230	0.362	−0.181	−0.460 to 0.095
	GEV	−2.239	0.075	1.611	−0.306	−0.589 to −0.027

Results of 2-sided independent-samples *t*-tests (frequentist and Bayesian approach) comparing the entire mixed chronic pain group with the healthy control group. *P*-values are FDR-adjusted. Mentioned in bold *P* < 0.05 and BF₁₀ > 3, indicating at least moderate evidence for the alternative hypothesis, and in italics BF₁₀ < 1/3, indicating at least moderate evidence for the null hypothesis. Median effect sizes (δ) and their respective 95% credible interval (CI) are reported.

BF₁₀, Bayes factor in favor of the alternative hypothesis; Freq. of occ., frequency of occurrence; GEV, global explained variance; Mean dur., mean duration; Time cov., time coverage.

time course of EEG activity as a sequence of a limited number of short stable topographies termed microstates. We applied microstate analysis to resting-state EEG activity and compared temporal characteristics of microstates between a large cohort of patients suffering from chronic pain and age- and sex-matched healthy control participants.

3.1. Definition of microstates A to E in patients and controls

We identified microstates using a standard two-step k-means clustering procedure.⁴² Five repetitions of the entire analysis showed reliable microstate definitions for the eyes-closed condition but very variable microstates for the eyes-open condition (Supplementary Figure 1, available at <http://links.lww.com/PAIN/B351>). Thus, all further analyses were restricted to the eyes-closed condition. For this condition, the clustering procedure consistently revealed 5 different microstates in both groups in 4 of 5 reruns. In a single rerun, only 4 microstates were found to be optimal for patients. Throughout the article, results and further analyses of a representative rerun with 5 microstates for both groups are presented. Results of additional reruns are presented in the supplementary material (available at <http://links.lww.com/PAIN/B351>).

In accordance with previous studies,^{6,8,11,26,27,34,35,63} the microstates were labeled as microstates A to E for both groups. Topographies for the representative rerun are depicted in **Figure 2A**. Together, these 5 microstates explained 81.05% and 81.08% of the variance across individuals for patients with chronic pain and healthy controls, respectively, which is in good accordance with previous studies.^{12,34,49} The high similarity of topographies between groups was confirmed by high spatial correlations (microstate A: *r* = 0.99, B: *r* = 1.00, C: *r* = 0.96, D: 0.93, and E: *r* = 0.92). In addition, TANOVAs revealed subtle group differences

between topographies hardly visible to the naked eye for microstates C to E (microstate A: *P* = 0.534, B: *P* < 0.091, C: *P* < 0.001, D: *P* < 0.001, and E: *P* < 0.001).

Taken together, the clustering procedures for both groups resulted in 5 microstate topographies, which were largely similar between groups.

3.2. Temporal characteristics of microstates in patients and controls

To investigate the dynamics of brain activity, we next analyzed whether the temporal characteristics of microstates differed between patients and healthy controls. To this end, 5 microstates were backfitted to the individual EEG time series by correlating microstate topographies with the EEG topographies at every time point for all reruns of the eyes-closed condition. This allowed to assign each time point to a microstate and, thus, to construe the EEG time series as time series of microstates.

We specifically calculated the mean duration, time coverage, frequency of occurrence, and global explained variance of each microstate. This was performed for each patient and each healthy control participant. We next compared these temporal microstate characteristics between groups for each rerun. Results are depicted in **Figure 2B** and **Table 2** for the representative rerun. Results for all other reruns can be found in Supplementary Table 1 (available at <http://links.lww.com/PAIN/B351>). Across reruns, microstate analysis consistently revealed strong evidence for changes in microstate D characteristics in patients compared with healthy participants. We found strong to very strong evidence for a lower time coverage, a lower frequency of occurrence, and lower global explained variance of microstate D in patients compared with controls in all 5 reruns (**Table 2**, Supplementary Table 1; all BF₁₀ > 10, all FDR-adjusted *P*-values < 0.011). In addition, results showed moderate to very strong

Table 3
Comparisons of transition probabilities between microstates for all patients with chronic pain (n = 101) compared with healthy controls (n = 88) in the eyes-closed condition (representative rerun).

	Mean trans. prob. patients with chronic pain	Mean trans. prob. HC	t	P	BF ₁₀	Median effect size (δ)	95% CI
From A to B	0.229	0.251	1.335	0.305	0.363	0.181	-0.095 to 0.460
From A to C	0.394	0.340	-2.273	0.071	1.727	-0.311	-0.594 to 0.031
From A to D	0.190	0.258	3.501	0.004	42.514	0.483	0.198 to 0.772
From A to E	0.183	0.147	-2.269	0.071	1.713	-0.310	-0.593 to -0.031
From B to A	0.244	0.218	-1.524	0.238	0.466	-0.207	-0.487 to 0.069
From B to C	0.385	0.360	-1.080	0.414	<i>0.273</i>	-0.146	-0.425 to 0.129
From B to D	0.187	0.273	4.548	<0.001	>100	0.633	0.342 to 0.927
From B to E	0.181	0.146	-2.046	0.105	1.102	-0.279	-0.561 to -0.001
From C to A	0.265	0.216	-2.470	0.071	2.647	-0.338	-0.622 to -0.058
From C to B	0.244	0.264	1.178	0.375	<i>0.302</i>	0.160	-0.116 to 0.438
From C to D	0.277	0.339	2.391	0.071	2.223	0.327	0.047 to 0.611
From C to E	0.211	0.178	-1.857	0.147	0.785	-0.253	-0.534 to 0.025
From D to A	0.192	0.191	-0.052	1	0.159	-0.007	-0.283 to 0.268
From D to B	0.177	0.230	3.673	0.003	73.594	0.508	0.222 to 0.797
From D to C	0.412	0.400	-0.498	0.860	<i>0.178</i>	-0.067	-0.344 to 0.208
From D to E	0.205	0.175	-1.513	0.238	0.459	-0.206	-0.485 to 0.071
From E to A	0.206	0.177	-2.250	0.071	1.647	-0.307	-0.590 to -0.028
From E to B	0.195	0.198	0.250	1	<i>0.163</i>	0.034	-0.242 to 0.310
From E to C	0.374	0.342	-1.508	0.238	0.456	-0.205	-0.485 to 0.072
From E to D	0.222	0.280	2.709	0.046	4.648	0.371	0.090 to 0.656

Results of 2-sided independent-samples *t*-tests (frequentist and Bayesian approach) comparing the entire mixed chronic pain group with the healthy control group. *P*-values are FDR-adjusted. Mentioned in bold *P* < 0.05 and BF₁₀ > 3, indicating at least moderate evidence for the alternative hypothesis, and in italics BF₁₀ < 1/3, indicating at least moderate evidence for the null hypothesis. Median effect sizes (δ) and their respective 95% credible interval (CI) are reported.

BF₁₀, Bayes factor in favor of the alternative hypothesis; HC, healthy controls; Mean trans. prob., mean transition probability.

evidence for a shorter mean duration of microstate D in patients in 4 of 5 reruns (Table 2; Supplementary Table 1, available at <http://links.lww.com/PAIN/B351>; BF₁₀ > 7, FDR-adjusted *P*-values < 0.016). In the fifth rerun, evidence was inconclusive (Supplementary Table 1, available at <http://links.lww.com/PAIN/B351>; rerun 4: BF₁₀ = 2.211, FDR-adjusted *P*-value = 0.089). Regarding the other microstates, a single rerun showed evidence for changes in the global explained variance of microstate C, while 2 reruns showed evidence for alterations in microstate E characteristics (Supplementary Table 1 for details, available at <http://links.lww.com/PAIN/B351>). However, these changes could not be replicated consistently.

For the representative rerun, we further investigated whether the sequences of microstates differed between groups. To this end, transition probabilities from each microstate to all other microstates were calculated. Mean transition probabilities for both groups as well as statistical results are presented in Table 3. In line with the analysis of temporal characteristics, we found moderate to very strong evidence for a lower transition probability from microstates A, B, and E to microstate D in patients compared with controls (Table 3; A to D: *P* = 0.004, BF₁₀ = 43; B to D: *P* < 0.001, BF₁₀ > 100; and E to D: *P* = 0.046, BF₁₀ = 5; FDR-adjusted *P*-values). In addition, healthy controls were more likely to transition from microstate D to microstate B than patients (Table 3; *P* = 0.003, BF₁₀ = 74; FDR-adjusted *P*-value). Evidence for differences of all other transition probabilities was either inconclusive or against a group difference (see Table 3 for details).

In summary, the analysis of the temporal dynamics of microstates revealed consistent evidence for a less predominant role of microstate D in eyes-closed resting-state brain activity of patients with chronic pain. Evidence for changes of the temporal characteristics of microstates other than D was inconsistent and could not be replicated across reruns of the analysis.

3.3. Relationships between temporal microstate characteristics and clinical characteristics

Having observed consistent evidence for changes of microstate D temporal characteristics in patients with chronic pain, we explored whether microstate D temporal measures were significantly related to clinical characteristics. To this end, we performed correlation analyses between the temporal measures of microstate D and clinical parameters of the patients. We specifically related microstate D characteristics obtained in the representative rerun to the current pain intensity, the SF-MPQ total pain score, as well as measures of depression (BDI) and medication (MQS). Frequentist statistics did not reveal significant correlations (Table 4; all *P* > 0.05, FDR-adjusted). This was confirmed using Bayesian statistics, which consistently provided moderate evidence for an absence of relations (Table 4; 1/10 < BF₁₀ < 1/3). Thus, the results did not provide evidence for relationships between microstate D temporal measures and clinical characteristics.

Table 4**Relationships between microstate D temporal measures and clinical parameters for all patients with chronic pain (n = 101) in the eyes-closed condition (representative rerun).**

	Current pain	SF-MPQ	BDI	MQS
Mean dur.				
Pearson's r	0.031	0.047	−0.020	0.127
<i>P</i>	0.927	0.927	0.956	0.927
BF ₁₀	<i>0.131</i>	<i>0.139</i>	<i>0.128</i>	<i>0.276</i>
95% CI	−0.163 to 0.224	−0.148 to 0.238	−0.213 to 0.174	−0.069 to 0.311
Time cov.				
Pearson's r	0.036	−0.035	−0.002	0.058
<i>P</i>	0.927	0.927	0.984	0.927
BF ₁₀	<i>0.133</i>	<i>0.133</i>	<i>0.125</i>	<i>0.147</i>
95% CI	−0.159 to 0.228	−0.227 to 0.160	−0.196 to 0.192	−0.136 to 0.248
Freq. of occ.				
Pearson's r	0.067	−0.072	0.084	−0.073
<i>P</i>	0.927	0.927	0.927	0.927
BF ₁₀	<i>0.156</i>	<i>0.161</i>	<i>0.176</i>	<i>0.162</i>
95% CI	−0.129 to 0.257	−0.261 to 0.124	−0.112 to 0.273	−0.261 to 0.122
GEV				
Pearson's r	0.046	−0.066	−0.011	0.059
<i>P</i>	0.927	0.927	0.927	0.927
BF ₁₀	<i>0.139</i>	<i>0.155</i>	<i>0.126</i>	<i>0.147</i>
95% CI	−0.149 to 0.237	−0.256 to 0.130	−0.204 to 0.183	−0.136 to 0.248

Pearson correlations (frequentist and Bayesian approach) were performed for microstate D temporal measures that had consistently shown evidence for differences between patients and controls across reruns of previous analyses. *P*-values are FDR-adjusted. Mentioned in italics BF₁₀ < 1/3, indicating at least moderate evidence for the null hypothesis.

95% CI, 95% credible interval; BF₁₀, Bayes factor in favor of the alternative hypothesis; BDI, Beck Depression Inventory; Freq. of occ., frequency of occurrence; GEV, global explained variance; Mean dur., mean duration; MQS, medication quantification scale; SF-MPQ, short-form McGill Pain Questionnaire; Time cov., time coverage.

3.4. Subgroup analyses

Since the patient group comprised patients with different types of chronic pain, we finally investigated whether our main finding of a less predominant role of microstate D in chronic pain could be replicated in different subgroups of patients. To this end, we repeated the definition of microstates and the investigation of their temporal characteristics in the eyes-closed condition for the 2 largest subgroups of patients, that is, patients suffering from chronic back pain and chronic widespread pain. For patients with chronic back pain, 5 reruns consistently revealed 5 microstates. For patients with chronic widespread pain, 4 of 5 reruns also revealed 5 microstates, while a single rerun revealed 6 microstates. Results of a representative rerun for each subgroup can be found in **Figures 3 and 4** and **Tables 5 and 6**. Results of additional reruns are provided in Supplementary Tables 2 and 3 (available at <http://links.lww.com/PAIN/B351>). To enable comparisons of temporal characteristics, further analyses were performed on the 5-microstate solutions of all reruns.

For patients with chronic back pain (representative rerun shown in **Figure 3**), all reruns consistently showed moderate to very strong evidence for a lower time coverage, frequency of occurrence, and global explained variance of microstate D in patients compared with controls (**Table 5**, Supplementary Table 2, available at <http://links.lww.com/PAIN/B351>; all BF₁₀ > 6, all FDR-adjusted *P*-values < 0.037). In addition, all but 1 reruns showed at least moderate evidence for a shorter mean duration of microstate D in patients (**Table 5**, Supplementary Table 2, available at <http://links.lww.com/PAIN/B351>; rerun 1: BF₁₀ = 0.308, FDR-adjusted *P*-value = 0.517; all other reruns: BF₁₀ > 3, all FDR-adjusted *P*-values < 0.038). With respect to the other microstates, some reruns additionally showed alterations in isolated measures of other microstates (see Supplementary Table 2 for details, available at <http://links.lww.com/PAIN/B351>), which were, however, not consistently replicated.

For patients with chronic widespread pain (representative rerun shown in **Figure 4**), Bayesian statistics showed moderate evidence against a group difference for most microstates and temporal characteristics (**Table 6**, Supplementary Table 3, available at <http://links.lww.com/PAIN/B351>). The only significant finding was an increased global explained variance of microstate B in patients compared with controls in a single rerun (Supplementary Table 3, rerun 4, available at <http://links.lww.com/PAIN/B351>), which was, however, not replicated across reruns.

Thus, although the small size of the subgroups has to be considered, our main finding of a less predominant role of microstate D could convincingly be replicated in patients with chronic back pain. By contrast, patients with chronic widespread pain did not show reliable microstate alterations.

4. Discussion

In this study, we investigated the dynamics of brain function in patients suffering from different types of chronic pain. To this end, we performed microstate analysis of resting-state EEG recordings in a large cohort of patients and age- and sex-matched healthy control participants. In both groups, resting-state brain activity could consistently be described as sequences of 5 microstates labeled A to E in the eyes-closed condition. However, a varying number of microstates were obtained in the eyes-open condition. Analyses of the temporal characteristics of these microstates in the eyes-closed condition revealed a decreased presence of microstate D in patients as compared to healthy participants. No consistent evidence for differences in other microstates was found. When investigating specific chronic pain pathologies, these findings were replicated for patients with chronic back pain. By contrast, patients with chronic widespread pain did not present microstate alterations. Thus, the present

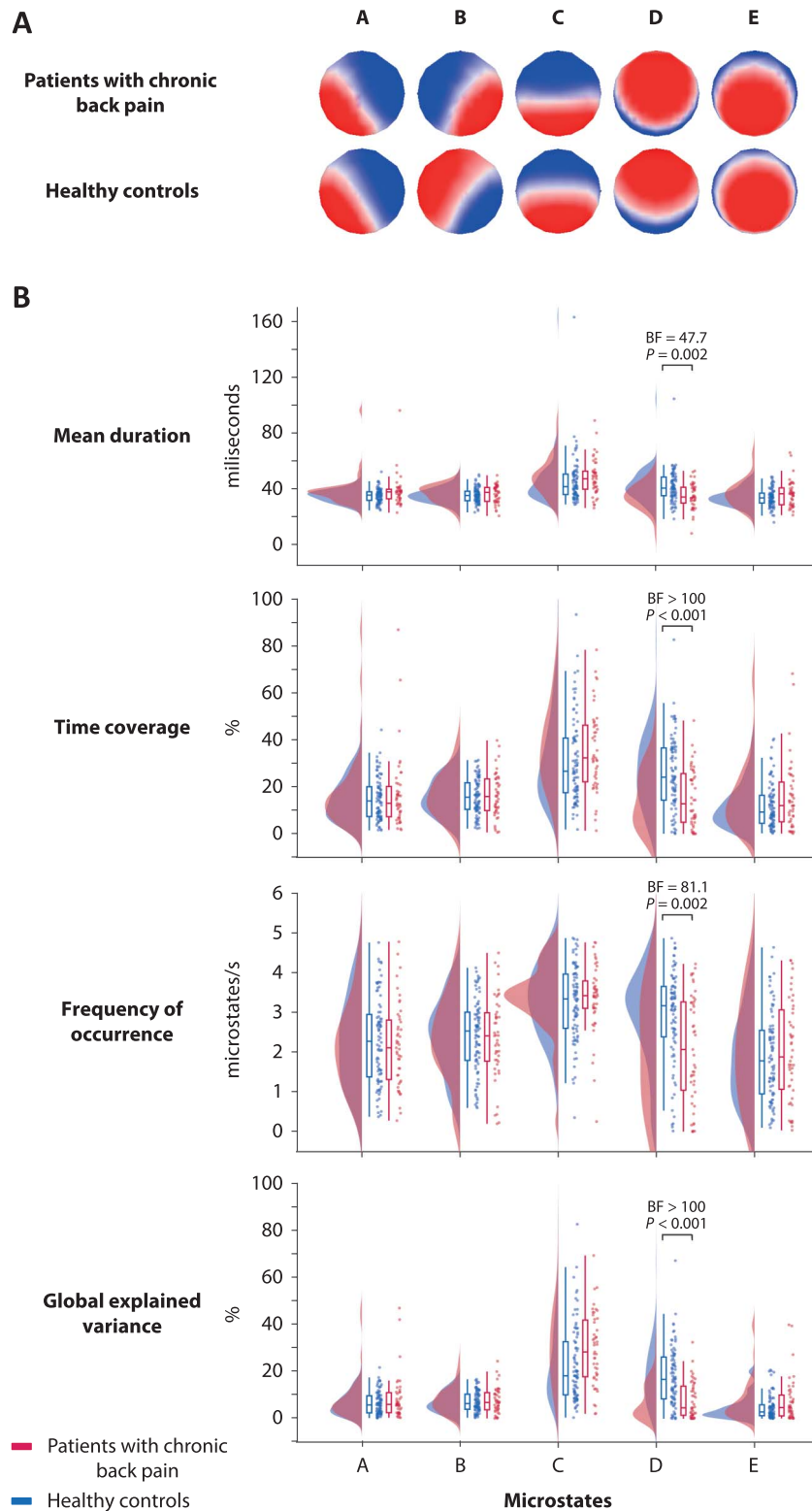


Figure 3. Microstate topographies and their temporal characteristics for patients with chronic back pain (n = 47) compared with healthy controls (n = 88) in the eyes-closed condition (representative rerun). (A) Microstate topographies were defined for the patients with chronic back pain and healthy controls separately. Microstates were labelled with the letters A to E according to previous literature.³⁴ (B) Temporal characteristics. Mean duration, time coverage, frequency of occurrence, and global explained variance of each microstate were calculated for each participant. Raincloud plots¹ show unmirrored violin plots displaying the probability density function of the data, boxplots, and individual data points. Boxplots depict the sample median as well as first (Q1) and third quartiles (Q3). Whiskers extend from Q1 to the smallest value within $Q1 - 1.5 \times \text{interquartile range (IQR)}$ and from Q3 to the largest values within $Q3 + 1.5 \times \text{IQR}$. BF, Bayes factor in favor of the alternative hypothesis.

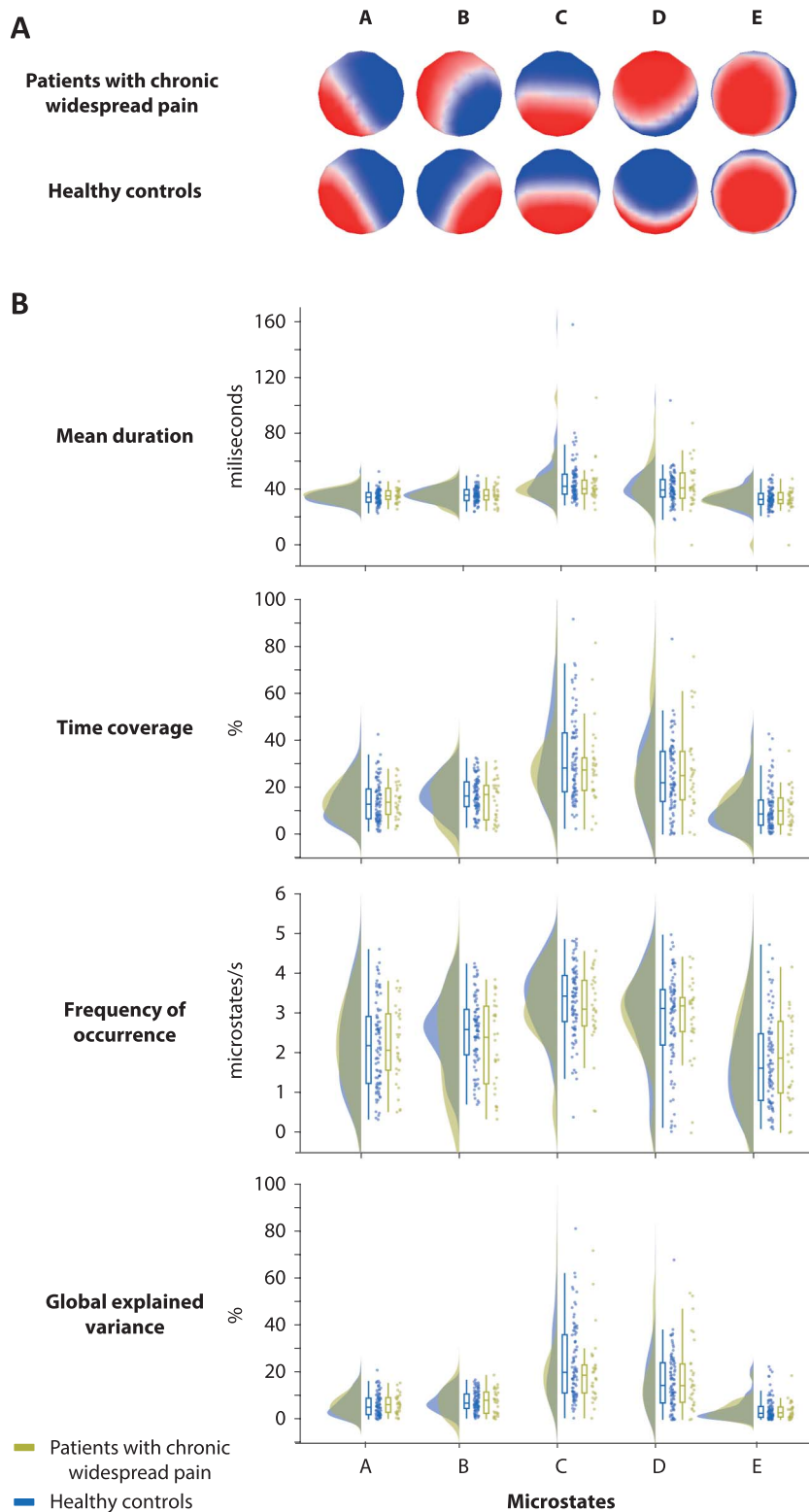


Figure 4. Microstate topographies and their temporal characteristics for patients with chronic widespread pain ($n = 30$) compared with healthy controls ($n = 88$) in the eyes-closed condition (representative rerun). (A) Microstate topographies were defined for the patients with chronic widespread pain and healthy controls separately. Microstates were labelled with the letters A to E according to previous literature.³⁴ (B) Temporal characteristics. Mean duration, time coverage, frequency of occurrence, and global explained variance of each microstate were calculated for each participant. Raincloud plots¹ show unmirrored violin plots displaying the probability density function of the data, boxplots, and individual data points. Boxplots depict the sample median as well as first (Q1) and third quartiles (Q3). Whiskers extend from Q1 to the smallest value within $Q1 - 1.5 \times$ interquartile range (IQR) and from Q3 to the largest values within $Q3 + 1.5 \times$ IQR.

Table 5

Comparisons of temporal microstate measures for patients with chronic back pain compared (n = 47) with healthy controls (n = 88) in the eyes-closed condition (representative rerun).

Microstate	Measure	t	P	BF ₁₀	Median effect size (δ)	95% CI
A	Mean dur.	2.234	0.093	1.802	0.368	0.026 to 0.719
	Time cov.	0.957	0.523	<i>0.291</i>	0.156	−0.180 to 0.496
	Freq. of occ.	−0.617	0.631	<i>0.229</i>	−0.100	−0.439 to 0.235
	GEV	1.524	0.259	0.549	0.249	−0.089 to 0.594
B	Mean dur.	0.868	0.552	<i>0.271</i>	0.141	−0.195 to 0.481
	Time cov.	0.431	0.702	<i>0.209</i>	0.070	−0.265 to 0.408
	Freq. of occ.	−0.274	0.784	<i>0.199</i>	−0.044	−0.382 to 0.291
	GEV	0.572	0.631	<i>0.223</i>	0.093	−0.242 to 0.431
C	Mean dur.	0.990	0.523	<i>0.300</i>	0.161	−0.175 to 0.502
	Time cov.	1.430	0.282	0.484	0.233	−0.104 to 0.578
	Freq. of occ.	0.664	0.631	<i>0.235</i>	0.108	−0.288 to 0.477
	GEV	2.219	0.093	1.749	0.366	0.023 to 0.717
D	Mean dur.	−3.540	0.002	47.788	−0.595	−0.956 to −0.240
	Time cov.	−4.114	<0.001	>100	−0.697	−1.063 to −0.336
	Freq. of occ.	−3.711	0.002	81.160	−0.625	−0.988 to −0.268
	GEV	−4.962	<0.001	>100	−0.849	−1.22 to −0.480
E	Mean dur.	2.000	0.118	1.160	0.329	−0.012 to 0.678
	Time cov.	1.672	0.215	0.678	0.274	−0.065 to 0.620
	Freq. of occ.	0.789	0.575	<i>0.255</i>	0.128	−0.207 to 0.468
	GEV	2.154	0.094	1.542	0.355	0.013 to 0.705

Results of 2-sided independent-samples *t*-tests (frequentist and Bayesian approach) comparing patients with chronic back pain with the healthy control group. *P*-values are FDR-adjusted. Mentioned in bold *P* < 0.05 and BF₁₀ > 3, indicating at least moderate evidence for the alternative hypothesis, and in italics BF₁₀ < 1/3, indicating at least moderate evidence for the null hypothesis. Median effect sizes (δ) and their respective 95% credible interval (CI) are reported.

BF₁₀, Bayes factor in favor of the alternative hypothesis; Freq. of occ., frequency of occurrence; GEV, global explained variance; Mean dur., mean duration; Time cov., time coverage.

findings describe microstate D-specific changes of the dynamics of brain function in eyes-closed resting-state EEG recordings of patients suffering from chronic pain. Beyond, they indicate that alterations of brain dynamics as measured by microstate analysis might be specific for certain types of chronic pain.

Our analyses reveal shorter mean duration, lower time coverage, fewer occurrences, and less explained variance of microstate D in patients compared with controls but no consistent alterations in other microstates. This pattern of results was found both when investigating the entire mixed chronic pain group or when specifically focusing on

Table 6

Comparisons of temporal microstate measures for patients with chronic widespread pain (n = 30) compared to healthy controls (n = 88) in the eyes-closed condition (representative rerun).

Microstate	Measure	t	P	BF ₁₀	Median effect size (δ)	95% CI
A	Mean dur.	0.871	0.954	<i>0.309</i>	0.160	−0.226 to 0.555
	Time cov.	−0.057	0.954	<i>0.222</i>	−0.010	−0.398 to 0.377
	Freq. of occ.	−0.086	0.954	<i>0.222</i>	−0.016	−0.404 to 0.371
	GEV	0.284	0.954	<i>0.229</i>	0.052	−0.334 to 0.441
B	Mean dur.	−0.293	0.954	<i>0.230</i>	−0.054	−0.443 to 0.333
	Time cov.	−1.173	0.954	0.405	−0.217	−0.615 to 0.171
	Freq. of occ.	−1.575	0.954	0.655	−0.293	−0.696 to 0.097
	GEV	−0.123	0.954	<i>0.223</i>	−0.022	−0.411 to 0.364
C	Mean dur.	−0.654	0.954	<i>0.267</i>	−0.120	−0.513 to 0.266
	Time cov.	−0.958	0.954	0.331	−0.177	−0.572 to 0.210
	Freq. of occ.	−1.066	0.954	0.365	−0.197	−0.594 to 0.190
	GEV	−0.982	0.954	0.338	−0.181	−0.577 to 0.206
D	Mean dur.	0.654	0.954	<i>0.267</i>	0.120	−0.266 to 0.513
	Time cov.	0.839	0.954	<i>0.302</i>	0.154	−0.232 to 0.549
	Freq. of occ.	0.114	0.954	<i>0.223</i>	0.021	−0.366 to 0.409
	GEV	0.717	0.954	<i>0.277</i>	0.132	−0.254 to 0.525
E	Mean dur.	−0.637	0.954	<i>0.264</i>	−0.117	−0.509 to 0.269
	Time cov.	−0.065	0.954	<i>0.222</i>	−0.012	−0.400 to 0.375
	Freq. of occ.	0.211	0.954	<i>0.226</i>	0.039	−0.348 to 0.427
	GEV	−0.454	0.954	<i>0.242</i>	−0.083	−0.474 to 0.303

Results of 2-sided independent-samples *t*-tests (frequentist and Bayesian approach) comparing patients with chronic widespread pain with the healthy control group. *P*-values are FDR-adjusted. Mentioned in italics BF₁₀ < 1/3, indicating at least moderate evidence for the null hypothesis. Median effect sizes (δ) and their respective 95% credible interval (CI) are reported.

BF₁₀, Bayes factor in favor of the alternative hypothesis; Freq. of occ., frequency of occurrence; GEV, global explained variance; Mean dur., mean duration; Time cov., time coverage.

the chronic back pain group. By contrast, no microstate alterations were found in patients suffering from chronic widespread pain. These findings are in contrast to the only study that applied microstate analysis to resting-state EEG recordings of patients suffering from chronic pain so far.²⁰ That study found a lower occurrence and time coverage of microstate C in eyes-open resting-state recordings of 43 patients suffering from chronic widespread pain. This difference between studies might at least in part be due to methodological differences. For example, the current study defined microstates separately for patients and controls, while the previous study defined microstates for both groups together. In addition, our sample size was smaller ($n = 30$ vs $n = 47$), and therefore, small effects might have been missed. Together, the 2 studies prompt further studies in larger groups of patients, ideally from different recording sites, to resolve these differences and to further clarify changes of microstates common to and different in distinct chronic pain populations.

Our observations further complement recent fMRI studies that have shown changes of the dynamics of brain function in chronic pain at ultra-low frequencies below 0.1 Hz.^{3,5,10} They extend this evidence by showing alterations of the dynamics of brain function at frequencies higher than 1 Hz, in line with the dynamic pain connectome concept.^{28,45}

Microstate analysis is an emerging tool for investigating the dynamics of brain activity. Although the functional interpretation of microstates is not fully clear yet, microstate analysis has been increasingly used to identify changes of brain dynamics in various neuropsychiatric diseases^{25,34} that have furthered the understanding of the pathology of these disorders. Beyond, alterations of microstates characteristics might be useful as clinical biomarkers. For instance, a recent study has identified the dynamics of microstates C and D as a promising candidate endophenotype for schizophrenia.¹² However, our data did not provide evidence for a correlation between alterations of microstate D and clinical characteristics. As the brain processes discriminating patients with chronic pain from healthy people differ from those encoding momentary pain intensity,^{3,32,54,59,64} the observed changes might reflect the abnormal disease state per se rather than its specific characteristics. Beyond, our analyses showed that results of our standard microstate analysis varied remarkably across repeated runs. This was in particular the case for patient data from the eyes-open condition, for which no stable optimal number of microstates could be obtained. This instability is likely due to higher variance and a stronger contamination of data by artifacts in eyes-open compared with eyes-closed resting-state recordings. Thus, future studies using microstate analyses should explicitly confirm reliability of findings.

Our most consistent and replicable finding was a reduced presence of microstate D in chronic pain. Microstate D has been related to attentional brain networks and functions (for reviews, see Refs. 34,51). In particular, microstate D has been associated with brain activity in frontoparietal regions,^{8,11} the dorsal attentional control network,⁴⁹ and focus-switching and attentional reorientation.³⁶ Interestingly, deficits of cognitive function and particularly of attentional switching have been extensively reported in patients suffering from chronic pain.³⁷ A common hypothesis is that pain competes with other stimuli for limited cognitive resources, thereby “demanding attention” and potentially impairing higher-order attentional control mechanisms.^{17,30,57} Thus, a decreased presence of microstate D might represent a neurophysiological correlate of altered attentional functioning in chronic pain. However, as we have not obtained direct measures of attentional functioning, we cannot directly test this hypothesis in this study. Future microstate studies on chronic pain might therefore include tasks and/or questionnaires assessing attentional functions.

Several limitations of the current study need to be discussed. First, the specificity of the decreased presence of microstate D for chronic pain is unclear. In particular, studies in patients suffering from schizophrenia^{12,47} and major depressive disorder³⁸ also showed a decreased presence of microstate D. However, investigating symptom- and disease-specificity of these findings is challenging. Substantial progress in this endeavor requires large samples of patients suffering from different neuropsychiatric symptoms and diseases, standardized assessments, and, ideally, sharing of data acquired at different sites. As a first step in that direction, we share data and code of this study in a standardized format with the research community. Second, comparisons of microstate topographies showed slight but statistically significant differences between patients and healthy controls. However, considering these subtle differences together with the overwhelming similarity of microstate topographies, the microstates of both groups likely capture the same underlying neural networks. Third, the causal relationship between altered microstate dynamics and chronic pain is unclear. First studies have shown that the dynamics of microstates can be changed by neurofeedback¹⁵ and noninvasive brain stimulation.⁵³ These approaches might thus be useful to prove the causal link between changes in microstate dynamics and neuropsychiatric disorders including chronic pain. Moreover, they highlight the potential utility of microstate dynamics as targets for neurofeedback- and/or brain stimulation-based treatments of chronic pain.

In conclusion, our findings provide evidence for altered and potentially pathology-specific dynamics of brain function in a large cohort of patients with chronic pain using EEG microstate analysis. We particularly observed alterations of microstate D. As this microstate has been associated with attentional brain networks and functions, changes of microstate D might relate to dysfunctional attentional processes in chronic pain. These results add to the understanding of the pathophysiology of chronic pain and indicate the need for future large-scale studies including patients suffering from chronic pain of different types.

Conflict of interest statement

The authors have no conflicts of interest to declare.

Acknowledgments

Supported by the Deutsche Forschungsgemeinschaft (PL 321/10-2, PL321/11-2, and PL321/13-1). E.S. May and C.Gil Ávila contributed to this work equally.

Appendix A. Supplemental digital content

Supplemental digital content associated with this article can be found online at <http://links.lww.com/PAIN/B351>.

Article history:

Received 2 October 2020

Received in revised form 10 March 2021

Accepted 17 March 2021

Available online 8 April 2021

References

- [1] Allen M, Poggiali D, Whitaker K, Marshall TR, Kievit RA. Raincloud plots: a multi-platform tool for robust data visualization. *Wellcome Open Res* 2019;4:63.
- [2] Baliki MN, Apkarian AV. Nociception, pain, negative moods, and behavior selection. *Neuron* 2015;87:474–91.

- [3] Baliki MN, Geha PY, Apkarian AV, Chialvo DR. Beyond feeling: chronic pain hurts the brain, disrupting the default-mode network dynamics. *J Neurosci* 2008;28:1398–403.
- [4] Beck AT, Steer RA, Brown G. Manual for the Beck Depression Inventory-II. San Antonio: Psychological Corporation, 1996.
- [5] Bosma RL, Kim JA, Cheng JC, Rogachov A, Hemington KS, Osborne NR, Oh J, Davis KD. Dynamic pain connectome functional connectivity and oscillations reflect multiple sclerosis pain. *PAIN* 2018;159:2267–76.
- [6] Bréchet L, Brunet D, Birot G, Gruetter R, Michel CM, Jorge J. Capturing the spatiotemporal dynamics of self-generated, task-initiated thoughts with EEG and fMRI. *NeuroImage* 2019;194:82–92.
- [7] Breivik H, Collett B, Ventafridda V, Cohen R, Gallacher D. Survey of chronic pain in Europe: prevalence, impact on daily life, and treatment. *Eur J Pain* 2006;10:287–333.
- [8] Britz J, Van De Ville D, Michel CM. BOLD correlates of EEG topography reveal rapid resting-state network dynamics. *NeuroImage* 2010;52:1162–70.
- [9] Brunet D, Murray MM, Michel CM. Spatiotemporal analysis of multichannel EEG: cartool. *Comput intelligence Neurosci* 2011;2011:813870.
- [10] Cheng JC, Rogachov A, Hemington KS, Kucyi A, Bosma RL, Lindquist MA, Inman RD, Davis KD. Multivariate machine learning distinguishes cross-network dynamic functional connectivity patterns in state and trait neuropathic pain. *PAIN* 2018;159:1764–76.
- [11] Custo A, De Ville DV, Wells WM, Tomescu MI, Brunet D, Michel CM. Electroencephalographic resting-state networks: source localization of microstates. *Brain Connectivity* 2017;7:671–82.
- [12] da Cruz JR, Favrod O, Roinishvili M, Chkonia E, Brand A, Mohr C, Figueiredo P, Herzog MH. EEG microstates are a candidate endophenotype for schizophrenia. *Nat Commun* 2020;11:3089.
- [13] Davis JF. Manual of surface electromyography. In: WADC Technical Report (59-184). Montreal: Aerospace Medical Laboratory, United States Air Force, 1959.
- [14] Davis KD, Aghaepour N, Ahn AH, Angst MS, Borsook D, Brenton A, Burczynski ME, Crean C, Edwards R, Gaudilliere B, Hergenroeder GW, Iadarola MJ, Iyengar S, Jiang Y, Kong JT, Mackey S, Saab CY, Sang CN, Scholz J, Segerdahl M, Tracey I, Veasley C, Wang J, Wager TD, Wasan AD, Pelleymounter MA. Discovery and validation of biomarkers to aid the development of safe and effective pain therapeutics: challenges and opportunities. *Nat Rev Neurol* 2020;16:381–400.
- [15] Diaz Hernandez L, Rieger K, Baenninger A, Brandeis D, Koenig T. Towards using microstate-neurofeedback for the treatment of psychotic symptoms in schizophrenia. A feasibility study in healthy participants. *Brain Topogr* 2016;29:308–21.
- [16] Dillmann U, Nilges P, Saile H, Gerbershagen HU. [Assessing disability in chronic pain patients. *Schmerz (Berlin, Germany)* 1994;8:100–10.
- [17] Eccleston C, Crombez G. Pain demands attention: a cognitive-affective model of the interruptive function of pain. *Psychol Bull* 1999;125:356–66.
- [18] Freynhagen R, Baron R, Gockel U, Tolle TR. painDETECT: a new screening questionnaire to identify neuropathic components in patients with back pain. *Curr Med Res Opin* 2006;22:1911–20.
- [19] Garrett DD, Samanez-Larkin GR, MacDonald SW, Lindenberger U, McIntosh AR, Grady CL. Moment-to-moment brain signal variability: a next frontier in human brain mapping? *Neurosci Biobehav Rev* 2013;37:610–24.
- [20] Gonzalez-Villar AJ, Trinanes Y, Gomez-Perretta C, Carrillo-de-la-Pena MT. Patients with fibromyalgia show increased beta connectivity across distant networks and microstates alterations in resting-state electroencephalogram. *NeuroImage* 2020;223:117266.
- [21] Harden RN, Weinland SR, Remble TA, Houle TT, Colio S, Steedman S, Kee WG. Medication Quantification Scale Version III: update in medication classes and revised detriment weights by survey of American Pain Society Physicians. *J Pain* 2005;6:364–71.
- [22] JASP Team (Version 0.14.1) [Computer software], 2020.
- [23] Jung TP, Makeig S, Humphries C, Lee TW, McKeown MJ, Iragui V, Sejnowski TJ. Removing electroencephalographic artifacts by blind source separation. *Psychophysiology* 2000;37:163–78.
- [24] Kennedy J, Roll JM, Schraudner T, Murphy S, McPherson S. Prevalence of persistent pain in the U.S. adult population: new data from the 2010 national health interview survey. *J Pain* 2014;15:979–84.
- [25] Khanna A, Pascual-Leone A, Michel CM, Farzan F. Microstates in resting-state EEG: current status and future directions. *Neurosci Biobehav Rev* 2015;49:105–13.
- [26] Koenig T, Lehmann D, Merlo MC, Kochi K, Hell D, Koukkou M. A deviant EEG brain microstate in acute, neuroleptic-naïve schizophrenics at rest. *Eur Arch Psychiatry Clin Neurosci* 1999;249:205–11.
- [27] Koenig T, Prichep L, Lehmann D, Sosa PV, Braeker E, Kleinlogel H, Isenhardt R, John ER. Millisecond by millisecond, year by year: normative EEG microstates and developmental stages. *NeuroImage* 2002;16:41–8.
- [28] Kucyi A, Davis KD. The dynamic pain connectome. *Trends Neurosci* 2015;38:86–95.
- [29] Kuner R, Flor H. Structural plasticity and reorganisation in chronic pain. *Nat Rev Neurosci* 2017;18:113.
- [30] Legrain V, Damme SV, Eccleston C, Davis KD, Seminowicz DA, Crombez G. A neurocognitive model of attention to pain: behavioral and neuroimaging evidence. *PAIN* 2009;144:230–2.
- [31] Lehmann D, Faber PL, Galderisi S, Herrmann WM, Kinoshita T, Koukkou M, Mucci A, Pascual-Marqui RD, Saito N, Wackermann J, Winterer G, Koenig T. EEG microstate duration and syntax in acute, medication-naïve, first-episode schizophrenia: a multi-center study. *Psychiatry Res Neuroimaging* 2005;138:141–56.
- [32] May ES, Nickel MM, Ta Dinh S, Tiemann L, Heitmann H, Voth I, Tölle TR, Gross J, Ploner M. Prefrontal gamma oscillations reflect ongoing pain intensity in chronic back pain patients. *Hum Brain Mapp* 2019;40:293–305.
- [33] Melzack R. The short-form McGill pain questionnaire. *PAIN* 1987;30:191–7.
- [34] Michel CM, Koenig T. EEG microstates as a tool for studying the temporal dynamics of whole-brain neuronal networks: a review. *NeuroImage* 2018;180:577–93.
- [35] Michel CM, Murray MM. Towards the utilization of EEG as a brain imaging tool. *NeuroImage* 2012;61:371–85.
- [36] Milz P, Faber PL, Lehmann D, Koenig T, Kochi K, Pascual-Marqui RD. The functional significance of EEG microstates-Associations with modalities of thinking. *NeuroImage* 2016;125:643–56.
- [37] Moriarty O, McGuire BE, Finn DP. The effect of pain on cognitive function: a review of clinical and preclinical research. *Prog Neurobiol* 2011;93:385–404.
- [38] Murphy M, Whitton AE, Decy S, Ironside ML, Rutherford A, Beltzer M, Sacchet M, Pizzagalli DA. Abnormalities in electroencephalographic microstates are state and trait markers of major depressive disorder. *Neuropsychopharmacology* 2020;45:2030–2037.
- [39] Murray MM, Brunet D, Michel CM. Topographic ERP analyses: a step-by-step tutorial review. *Brain Topography* 2008;20:249–64.
- [40] Nishida K, Morishima Y, Yoshimura M, Isotani T, Irisawa S, Jann K, Dierks T, Strik W, Kinoshita T, Koenig T. EEG microstates associated with salience and frontoparietal networks in frontotemporal dementia, schizophrenia and Alzheimer's disease. *Clin Neurophysiol* 2013;124:1106–14.
- [41] Oostenveld R, Fries P, Maris E, Schoffelen JM. FieldTrip: open source software for advanced analysis of MEG, EEG, and invasive electrophysiological data. *Comput intelligence Neurosci* 2011;2011:156869.
- [42] Pascual-Marqui RD, Michel CM, Lehmann D. Segmentation of brain electrical activity into microstates: model estimation and validation. *Ieee T Bio-med Eng* 1995;42:658–65.
- [43] Pernet CR, Appelhoff S, Gorgolewski KJ, Flandin G, Phillips C, Delorme A, Oostenveld R. EEG-BIDS, an extension to the brain imaging data structure for electroencephalography. *Sci Data* 2019;6:103.
- [44] Ploner M, May ES. Electroencephalography and magnetoencephalography in pain research - current state and future perspectives. *PAIN* 2018;159:206–11.
- [45] Preti MG, Bolton TA, Van De Ville D. The dynamic functional connectome: state-of-the-art and perspectives. *NeuroImage* 2017;160:41–54.
- [46] Rice AS, Smith BH, Blyth FM. Pain and the global burden of disease. *PAIN* 2016;157:791–6.
- [47] Rieger K, Diaz Hernandez L, Baenninger A, Koenig T. 15 Years of microstate research in schizophrenia - where are we? A meta-analysis. *Front Psychiatry* 2016;7:22.
- [48] Schumacher J, Peraza LR, Firbank M, Thomas AJ, Kaiser M, Gallagher P, O'Brien JT, Blamire AM, Taylor JP. Dysfunctional brain dynamics and their origin in Lewy body dementia. *Brain* 2019;142:1767–82.
- [49] Seitzman BA, Abell M, Bartley SC, Erickson MA, Bolbecker AR, Hetrick WP. Cognitive manipulation of brain electric microstates. *NeuroImage* 2017;146:533–43.
- [50] Selim AJ, Rogers W, Fleishman JA, Qian SX, Fincke BG, Rothendler JA, Kazis LE. Updated U.S. Population standard for the veterans RAND 12-item health survey (VR-12). *Qual Life Res* 2009;18:43–52.
- [51] Shaw SB, Dhindsa K, Reilly JP, Becker S. Capturing the forest but missing the trees: microstates inadequate for characterizing shorter-scale EEG dynamics. *Neural Comput* 2019;31:2177–211.
- [52] Spielberger CD, Gorsuch RL, Lushene R, Vagg PR, Jacobs GA. Manual for the State-Trait Anxiety Inventory. Palo Alto: Consulting Psychologists Press, 1983.
- [53] Sverak T, Albrechtova L, Lamos M, Rektorova I, Ustohal L. Intensive repetitive transcranial magnetic stimulation changes EEG microstates in schizophrenia: a pilot study. *Schizophr Res* 2018;193:451–2.

- [54] Ta Dinh S, Nickel MM, Tiemann L, May ES, Heitmann H, Hohn VD, Edenharter G, Utpadel-Fischler D, Tolle TR, Sauseng P, Gross J, Ploner M. Brain dysfunction in chronic pain patients assessed by resting-state electroencephalography. *PAIN* 2019;160:2751–65.
- [55] Tomescu MI, Rihs TA, Becker R, Britz J, Custo A, Grouiller F, Schneider M, Debbané M, Eliez S, Michel CM. Deviant dynamics of EEG resting state pattern in 22q11.2 deletion syndrome adolescents: a vulnerability marker of schizophrenia? *Schizophrenia Res* 2014;157:175–81.
- [56] Tomescu MI, Rihs TA, Rochas V, Hardmeier M, Britz J, Allali G, Fuhr P, Eliez S, Michel CM. From swing to cane: sex differences of EEG resting-state temporal patterns during maturation and aging. *Develop Cogn Neurosci* 2018;31:58–66.
- [57] Torta DM, Legrain V, Mouraux A, Valentini E. Attention to pain! A neurocognitive perspective on attentional modulation of pain in neuroimaging studies. *Cortex* 2017;89:120–34.
- [58] Tracey I, Woolf CJ, Andrews NA. Composite pain biomarker signatures for objective assessment and effective treatment. *Neuron* 2019;101:783–800.
- [59] Tu Y, Fu Z, Mao C, Falahpour M, Gollub RL, Park J, Wilson G, Napadow V, Gerber J, Chan ST, Edwards RR, Kaptchuk TJ, Liu T, Calhoun V, Rosen B, Kong J. Distinct thalamocortical network dynamics are associated with the pathophysiology of chronic low back pain. *Nat Commun* 2020;11:3948.
- [60] Turk DC, Wilson HD, Cahana A. Treatment of chronic non-cancer pain. *Lancet* 2011;377:2226–35.
- [61] Winkler I, Debener S, Muller KR, Tangermann M. On the influence of high-pass filtering on ICA-based artifact reduction in EEG-ERP. *Conf Proc 2015;2015:4101–5*.
- [62] Yekutieli D, Benjamini Y. Resampling-based false discovery rate controlling multiple test procedures for correlated test statistics. *J Stat Plann Inference* 1999;82:171–96.
- [63] Zanesco AP, King BG, Skwara AC, Saron CD. Within and between-person correlates of the temporal dynamics of resting EEG microstates. *Neuroimage* 2020;211:116631.
- [64] Zhang B, Jung M, Tu Y, Gollub R, Lang C, Ortiz A, Park J, Wilson G, Gerber J, Mawla I, Chan ST, Wasan A, Edwards R, Lee J, Napadow V, Kaptchuk T, Rosen B, Kong J. Identifying brain regions associated with the neuropathology of chronic low back pain: a resting-state amplitude of low-frequency fluctuation study. *Br J Anaesth* 2019;123:e303–11.